

INVITED PAPER

Polarisation independent liquid crystal lenses and contact lenses using embossed reactive mesogens

J. Cliff Jones SID Senior Member¹  | Markus Wahle¹  | James Bailey² | Tom Moorhouse² | Benjamin Snow³ | Joe Sargent SID Member³

¹School of Physics and Astronomy, University of Leeds, Leeds, UK

²Dynamic Vision Systems Ltd, Leeds Innovation Centre, Leeds, UK

³Merck Chemicals Ltd, Southampton, UK

Correspondence

J. Cliff Jones, School of Physics and Astronomy, University of Leeds, Woodhouse Lane, Leeds, LS2 9JT, UK.
Email: j.c.jones@leeds.ac.uk

Funding information

Merck Darmstadt; Merck; Engineering and Physical Sciences Research Council, Grant/Award Number: EP/L015288/2

Abstract

Liquid crystal lenses have promise in optical systems owing to their tunability combined with low electrical power, cost, and weight. A good example of such a system is switchable contact lenses for the correction of age-related presbyopia. Sufficiently large phase modulation can be done using nematic liquid crystals in a meniscus lens configuration. However, the birefringent materials are inherently polarisation dependent, usually requiring orthogonal polarisations to be focussed separately. A novel method is presented for producing polarisation independent lenses based on reactive mesogens. Results are presented for a 2-level and 3-level diffractive Fresnel lenses, and the promise of the technique for use in refractive lenses such as contact lenses is discussed.

KEYWORDS

adaptive optics, embossing, liquid crystal lens, nematic, reactive mesogens, switchable contact lens

1 | INTRODUCTION

The low voltages required to modulate the optical phase of nematic liquid crystals has long suggested their use for adaptive optical elements, such as switchable gratings, prisms, and lenses.¹ Many types of lens have been suggested,² including both refractive and diffractive types, where the variation of phase is induced through changes of shape, electric field, or alignment of the liquid crystal director. Nematic liquid crystals are birefringent materials, with cylindrical symmetry and a single optic axis. Hence, field induced optical phase changes only occur for light polarised in the plane of the optic axis and parallel to the extraordinary refractive index. Light polarised perpendicular to the optic axis experiences the ordinary refractive index regardless of the

voltage applied. This is not an issue for the many applications where polarised light is used, for example, to provide different images for the left and right eye.³ However, for switchable contact lenses^{4–7} and camera lenses,⁸ it is important that lenses operate with unpolarised light and high optical efficiency.

The simplest adaptive contact lens uses a nematic liquid crystal contained within an electrically active cavity with a varying thickness Δd to form a meniscus lens, as shown in Figure 1.^{4,5} The refractive index of the lens substrate is matched to the ordinary index of the liquid crystal so that there is no lensing effect for the vertical state. In the horizontal state, light polarised parallel to the extraordinary index is not matched, and lensing occurs, with a focussing strength ΔP given by Bailey et al.⁷:

This is an open access article under the terms of the Creative Commons Attribution License, which permits use, distribution and reproduction in any medium, provided the original work is properly cited.

© 2020 The Authors. Journal of the Society for Information Display published by Wiley Periodicals, Inc. on behalf of Society for Information Display

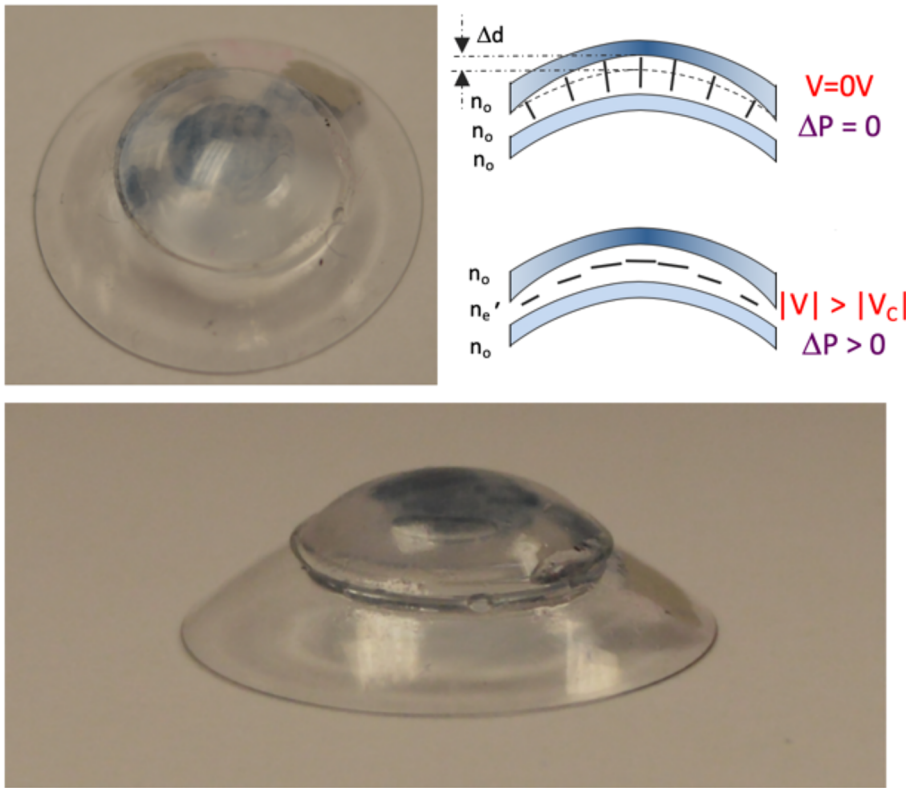


FIGURE 1 A switchable contact lens using a nematic liquid crystal (LC) from Dynamic Vision Systems.⁴⁻⁷ There are a variety of potential geometries including the positive meniscus lens arrangement using homeotropically aligned nematic^{5,6} as shown in the inset

$$\Delta P = \Delta n' \left(\frac{1}{r_2} - \frac{1}{r_1} \right), \quad (1)$$

where r_1 and r_2 the inner and outer radii of curvature of the lens, respectively, and $\Delta n'$ is the difference in refractive index induced by the applied field, which approaches the birefringence Δn of the liquid crystal for high fields.

A variety of arrangements are possible,⁷ such as the homeotropically aligned version with a negative $\Delta \epsilon$ nematic material⁵ shown in Figure 1. Here, the lens is a positive meniscus shape, with the liquid crystal at its thickest at the central symmetry axis of the lens. Given that calamitic liquid crystals all have a positive birefringence, this arrangement gives a positive change in the optical power, ΔP . In practice, this lens operates with rubbed

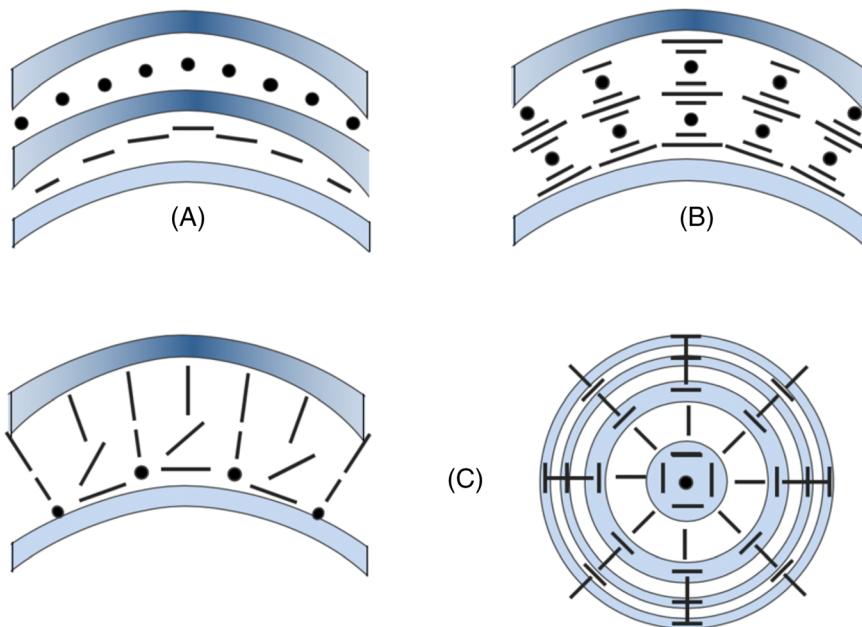


FIGURE 2 Previous approaches for achieving polarisation independence: A, dual chamber; B, near-infrared light (NIR) cholesteric or a Blue-Phase liquid crystal (LC); C, alternating orthogonally photo-aligned Fresnel zones

homeotropic layers to give the uniformly aligned director configuration, either with planar homogenous or axial homogenous alignment of the director in the fully switched state.⁷

It is important to recognise that the presbyope's eye lens is still operational but has a range inhibited by increased rigidity of the lens caused by natural ageing. Thus, the contact lens will often include a static lens for the correction of distance vision and that the switchable contact element is only required to provide an extra +2 to +2.5 dioptre of optical power ΔP . For a typical liquid crystal with $\Delta n \approx 0.25$, the change in cavity spacing across the an 8-mm-diameter contact lens is $\Delta d \approx 25 \mu\text{m}$ to achieve the typical focal correction needed for the correction of presbyopia. Thus, the simple meniscus type is well suited for contact lenses, since the optical response time for nematic of this cell gap is significantly lower than the target correction speed of 1 s. This type of lens is currently being made by the UK company Dynamic Vision Systems Ltd (DVS).

Currently, multi-focal contact lenses use areas designed for correcting near and far vision. The user needs to adapt to seeing two different focal points after a period of use. Any adaptive contact lens solution needs to provide far higher discrimination between the two focusses, which are corrected by the liquid crystal and that by the static contact lens (or none at all, if far field vision is not corrected). This is in addition to fulfilling other specifications including operation across the optical wavelength range with optical clarity, and with a maximum thickness of only 300 μm . Some of the requirements

for the liquid crystal are less stringent than for other applications. Of course, a standard shipping temperature range is required, but operating temperatures are between 35°C to 37°C. Although the cone of visual attention is 114°, the central visual field is less than 8°⁹ and substantially lower than that required for most liquid crystal applications. An essential requirement for any ophthalmic lens, including contact lenses, is to focus the light independently of polarisation. Not only is this critical for viewing modern display devices, but any reduction in the contrast of the focussed to unfocussed light would not be competitive with existing multi-focus contact lenses. Some of the previous methods for achieving this insensitivity are illustrated in Figure 2. The typical method for this is to use two orthogonally aligned lenses in series^{4,10,11} (Figure 2a). However, this adds increased optical loss, cost, weight, and manufacturing complexity. Alternatively, electric field effects that are inherently polarisation-independent may be used, such as those that occur in cholesteric liquid crystals with helical pitches that selectively reflect in the near-infrared,¹² (Figure 2b) or the Kerr effect in Blue-Phase liquid crystals.^{13,14} However, in addition to being more difficult to align and having higher switching fields, these modes have a fundamentally lower phase modulation, with the maximum phase retardation being proportional to $\Delta n/2$ rather than Δn as for the nematic type. Because the response time increases with square of cell gap, this would lead to almost a 4-fold decrease of speed for the cholesteric and would prohibit the use of a simple meniscus lens type for contact lenses. Other polarisation independent modes

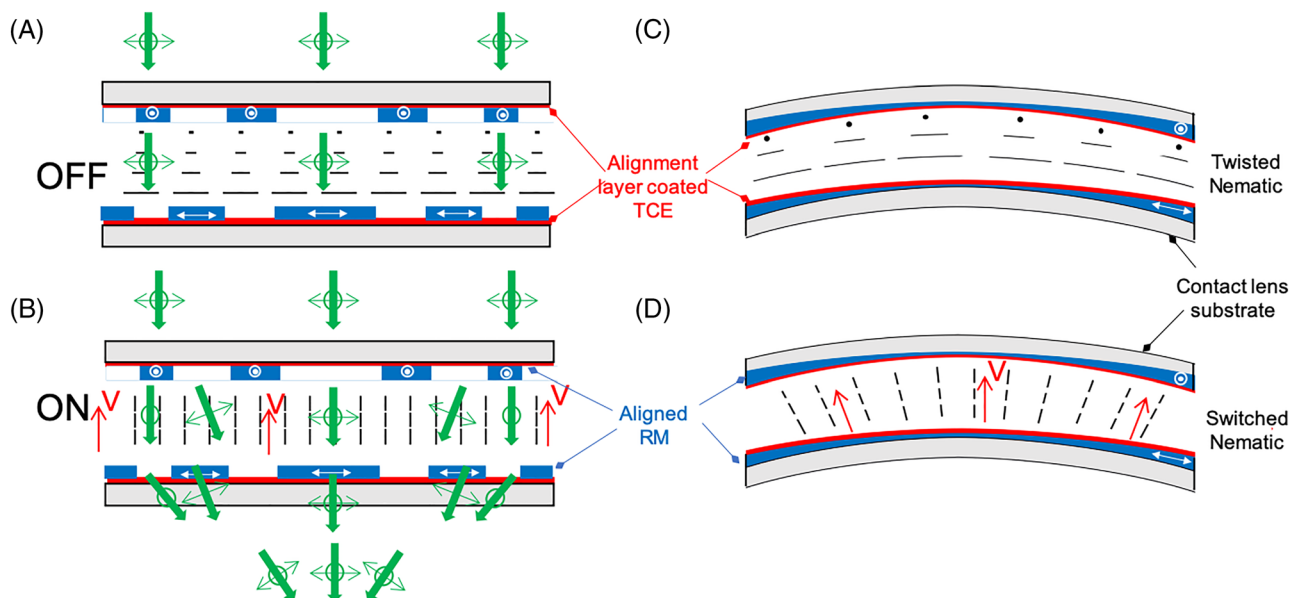


FIGURE 3 Operating principle of the proposed lenses.¹⁶ A simple 2-level diffractive Fresnel lens is shown on a flat substrate in both the A, field OFF and B, field ON states. The operating principle for an adaptive contact lens operating in this same fashion is shown for the field OFF, C, and ON, D, states. RM, reactive mesogen; TCE,

include diffractive lenses with alternating alignment directions in the Fresnel zones¹⁵ (Figure 2c). However, the fabrication is rather complex for a contact lens, and the resulting diffraction-based lens is highly chromatic and again of low efficiency due to the lower effective birefringence.

2 | NOVEL DESIGN FOR NEMATIC POLARISATION INDEPENDENT LENS

The objective of the present work is to design an arrangement for a conventional nematic liquid crystal that could produce polarisation independent operation for either multi-level diffractive or refractive optical structures, producing high efficiency lenses operating at lower voltages. The approach taken was to form optical

structures on the internal sides of the liquid crystal device from birefringent materials that are index matched to the contacting liquid crystal and orthogonal to each other.¹⁶ Each refractive or diffractive lens structure is formed in a parallel-aligned reactive mesogen on to the internal surfaces of the liquid crystal lens, deposited directly onto the electrodes. The device is constructed with two such lenses opposing each other, and the optic axes of the birefringent material are arranged to be orthogonal, with both ordinary and extraordinary refractive indices matched to those of the contacting nematic. The quiescent state of the liquid crystal can either be a uniform birefringent waveplate in the half-wave plate condition or, preferably, a 90° twisted nematic (TN) arrangement, as shown in Figure 3. The latter arrangement ensures that the lens operates over a wide wavelength and angle of incidence range and is less sensitive to fabrication errors.

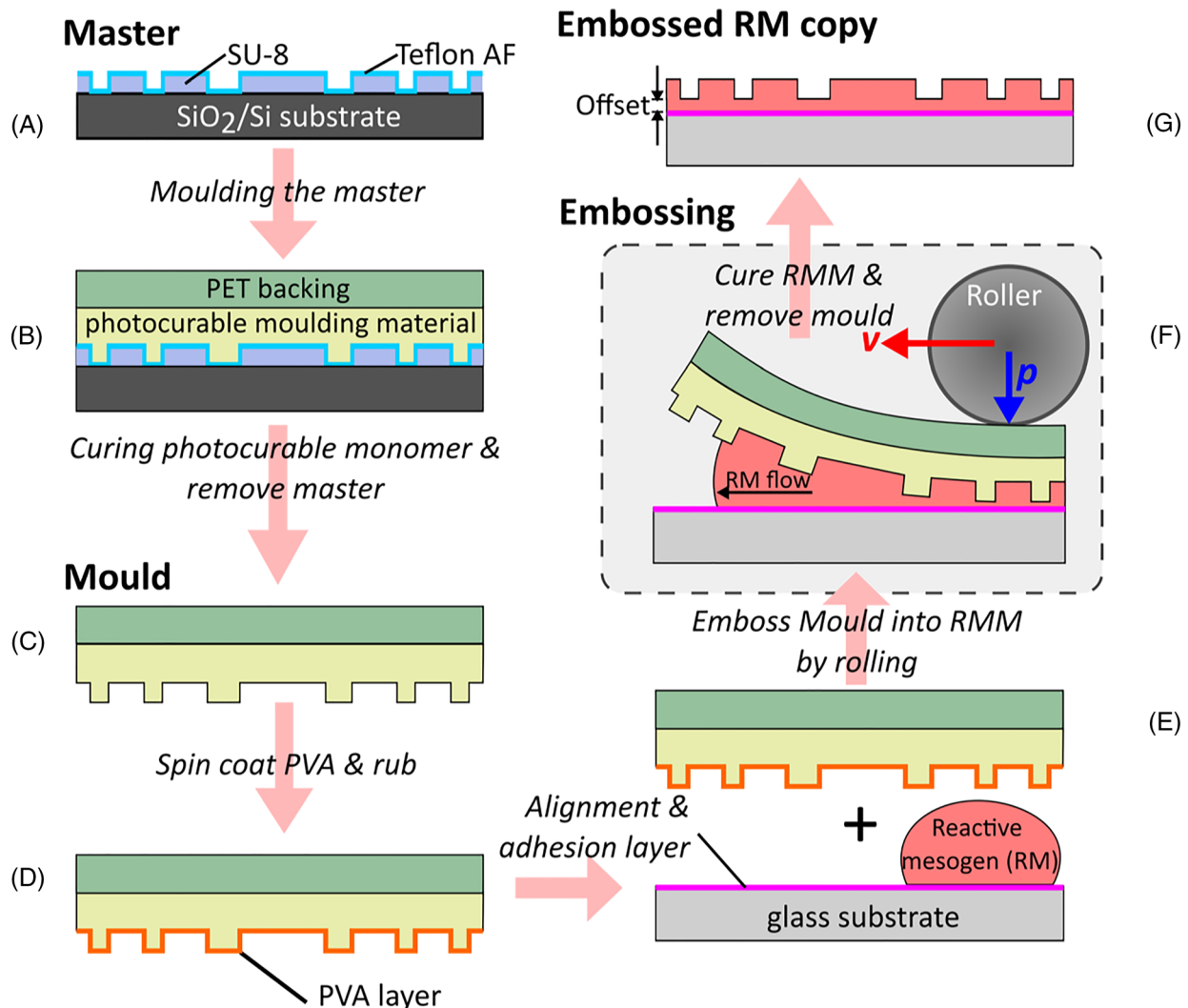


FIGURE 4 Method of copying the lens onto a backing film and then embossing it onto the indium tin oxide (ITO) coated liquid crystal lens substrate using embossing. PET, polyethylene terephthalate; PVA, polyvinyl acetate

Without a field applied, the nematic director remains aligned parallel to the birefringent optic axes on both upper and lower lens surfaces, and is therefore index matched for any polarisation: lensing does not occur (Figure 3A). However, the polarisation state is rotated through 90° due to the TN structure. This ensures that light of a particular polarisation is rotated as it is transmitted through the liquid crystal, so that the index matching condition is met on the opposite, orthogonal lens surface. Polarisation conversion stops when the positive $\Delta\epsilon$ liquid crystal is switched by the applied field; the index matching condition is then lost for the extraordinary polarisation at the first incident surface, which exhibits some component of the extraordinary refractive index. The upper lens then focusses this polarisation, whilst the other polarisation is transmitted through the liquid crystal without being focussed. When the first polarisation is incident on the lower lens substrate, its polarisation plane is parallel to the ordinary index, and no further optical effect occurs. However, the other polarisation, unaffected by the first substrate, now experiences the unmatched refractive index condition and hence undergoes lensing at the second surface. In this fashion, lensing for orthogonal polarisations occurs separately at the two surfaces. For diffractive lenses, complementary structures can be used opposite each other, as shown in Figure 3A,B. This ensures that the electric field is approximately uniform across the device, and both polarisations are switched to the same extent for a given applied field. Figure 3C,D shows how the arrangement is

adapted for a meniscus type contact lens. In this example, the electrodes are better deposited on top of the reactive mesogen (RM) lens, together with an appropriate alignment layer. However, the principles for both diffractive and refractive lens types remain the same. In this work, the basic principle is proven using a diffractive lens, not suited for use in a contact lens. This is followed by considering how the approach would be applied to an adaptive contact lens.

3 | EMBOSSED METHOD OF REPLICATION IN BIREFRINGENT STRUCTURES

A simple method for creating birefringent lenses onto the inner surface of an LCD is to use RMs. The best optical properties and simplest geometry result if the liquid crystal is in direct contact with the RM so that the liquid crystal aligns with the polymerised director of the RM and no extra alignment layer is required. This arrangement requires the device electrodes to be below the passive birefringent element, in the conventional position for an LCD. However, any unwanted offset between the electrodes and the optical structure causes severe electrical losses in the device. More importantly, any small variations of this offset cause variations in the applied field and hence uniformity of the lens with applied field. Offset can be minimised using the embossing approach used previously to construct a zenithal bistable LCD^{17–19}

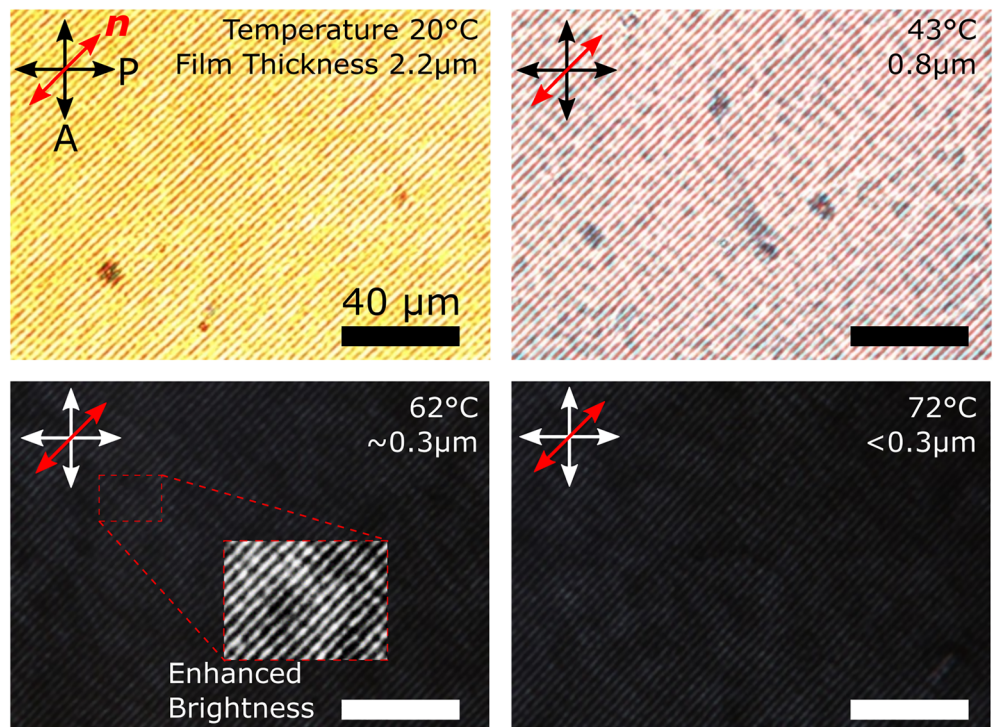


FIGURE 5 Achieving zero-offset in RMM 1850 grating using elevated temperature of the embossing plate. The offsets shown were determined by Dektak, and are consistent with values determined from birefringence colour and from cross-sectional scanning electron microscopy (SEM)

(as shown in Figure 4G). This encompasses copying a master structure into a negative on a flexible backing film, which is then used to emboss the required structure onto the inside of the liquid crystal.

The master lens is first defined by a conventional method, such as lithography, lathing or moulding (Figure 4A). The master is coated with a CYTOP or Teflon layer to assist release from subsequent copies. The master is copied into a photocurable or thermosetting resin on a polyethylene terephthalate (PET) backing film (Figure 4B). The resulting inverse lens structure (Figure 4C) has a surface alignment direction imposed, either through rubbing or photoalignment as shown in Figure 4D. The device substrate also has a thin alignment layer deposited onto the indium tin oxide (ITO) electrodes (Figure 4E). Uncured RM is placed at one side of the substrate, and the film is then pressed onto RM and passed from one side of the device as shown in Figure 4F. The highest features of the lens structure touch the alignment layer, with the liquid RM flowing into the gaps that form the lens. In this fashion, the unused RM is pushed ahead of the roller, rather than contributing to offset under the structure.¹⁷ After curing, the RM remains aligned by both the substrate and the surface of the film to give a uniformly birefringent lens (Figure 4G).

The target design for the Fresnel lens has a focal length of 200 mm at 594 nm and an outer diameter of 5 mm. The reactive mesogen used was RMM 1850, which was found to have ambient temperature refractive indices

of $n_e = 1.654$ and $n_o = 1.510$ at 594 nm, measured using a 45° prism. Thus, the height of the SU-8 master features was designed to be 2.1 μm to obtain the π -phase shift necessary for the diffractive structure. There was little density change on curing the RM, and so, the amplitude and refractive indices of the cured polymer were taken to be unchanged. The viscosity of the RM is higher than that used for conventional embossing of photopolymers and required the temperature of the embossing plate to be elevated to allow suitably low pressures and higher speeds to be used. Figure 5 shows the calibration of the embossing temperature made for a sub-micron pitch grating, indicating that temperatures above 70°C were suitable for achieving no offset in an aligned RM. It should be observed that this temperature was below the clearing point, $T_{NI} = 86.5^\circ\text{C}$.

Complementary versions of the zone plates were made, where all odd zones are formed from RM in one version and in the even zones for the other. The Fresnel zone plate masters were manufactured using direct laser write. SU-8-2025 (38% in Cyclopentanone) was spin coated onto a silicon wafer at 500 rpm (100 rpm/s) for 10 s and 1000 rpm (300 rpm/s) for 40 s, where the dilution of the neat SU-8 was used to obtain the desired film thickness. The sample soft-baked for 30 min at 30°C. The writing process is performed using a Direct Write Laser system from Durham Magneto Optics (Microwriter ML3 Pro) using a 375-nm laser with a nominal dose of 3000 mJ/cm². The post exposure bake was done at 50°C for 30 min, after which the master was developed by spin-

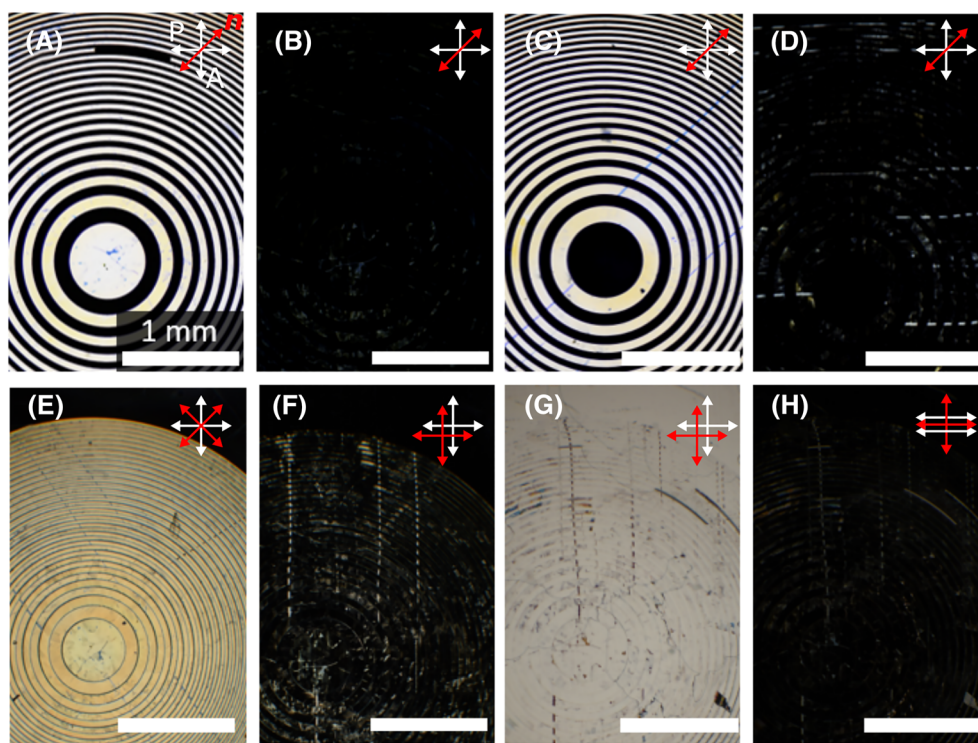


FIGURE 6 Micrographs of single substrates: A-D, and the assembled cell: E, F, unfilled; G, H, unfilled. White arrows indicate the polariser and analyser orientation, Red arrows indicate the director orientation

coating SU-8 developer followed by rinsing with isopropyl alcohol (IPA) and hard baking at 180°C for 1 h. The desired feature height of 2.1 μm was verified by measuring the surface profile (Dektak XT). Good release during the subsequent copying processes was ensured by spin-coating the master with the low surface energy surfactant Teflon AF1600 (1.7%) in FC40 (both Sigma Aldrich) at 500 rpm (100 rpm/s) for 10 s and 3000 rpm (300 rpm/s) for 40s and dried at 180°C for 15 min.

The isotropic resin that is used to mould the master consists of 45% 5,7-Hexamethylene diacrylate (HDDA) (Sigma Aldrich), 15% Trimethylolpropane triacrylate (TMPTA) (Sigma Aldrich) and 40% Actilane 420. The resin was deposited on the master, topped with flexible 125- μm thick PET film (Melinex 506, HIFI films) and then cured at 10-mW/cm² UVA for 10 min. After curing, the film is lifted off, and the cured resin adheres to the plastic backing. The mould is exposed to UV-ozone for 5 min (T10X10/OES, UVOCS) before spin coating polyvinyl acetate (PVA) solution (1% in H₂O) at 500 rpm (100 rpm/s) for 10 s and 1500 rpm (300 rpm/s) for 30 s. The PVA layer was dried at 90°C for 10 min and at 130°C for 30 min. In a final step, the mould is rubbed using a rubbing machine equipped with a velvet cloth in the standard fashion used for LCD production.

For the embossing, a droplet of reactive mesogen mixture RMM1850 (Merck Chemicals Ltd) was deposited onto the ITO substrate that had been pre-coated with the rubbed alignment layer SE 3510 (Nissan Chemicals). The rubbed mould was placed on top with care taken to ensure parallel alignment directions. The embossing process was performed at a base plate temperature 85°C, 4.5 bar of roller pressure and substrate speed of 6.5 mm/s, where the steel roller is 10 cm in diameter and covered with a shore hardness 70 rubber coating.¹⁷ After embossing, the sample was cooled to room temperature within a period of 5 min. The sample was UV-cured with a UVA intensity of 10 mW/cm² (measured with radiometer RM-12, Opsytec Dr Groebel GmbH) for 10 min.

Finally, the film was removed, leaving behind the reproduced structure. Note, the completed plate has only a single alignment layer underneath the embossed RM lens; uniform alignment throughout the RM is achieved by rubbing the film, which is then subsequently discarded. Uniform alignment of RM structures up to 50 μm thick have been achieved using this method.

The normal and complementary Fresnel zone plate substrates are assembled into a 23- μm -spaced cell such that the directors form a 90° angle. Placement was performed by hand whilst viewing under a stereoscope to ensure good positioning of the structures. The cell gap was controlled using Mylar spacers of appropriate thickness. The cell is sealed on three of the four sides to enable vacuum filling. This method of filling is necessary as capillary filling usually leads to air bubbles being trapped in the cell. The cell is filled with nematic liquid crystal MLC-6204-000, which has a high $\Delta\epsilon$ ($\approx +30$ at 25°C) and refractive indices almost equivalent to those measured for RMM1850.

4 | RESULTS FOR A POLARISATION INDEPENDENT DIFFRACTIVE FRESNEL LENS

An example of two embossed substrates and the subsequently assembled cell made from those substrates is shown in Figure 6. Here, we chose to produce the normal structure (Figure 6A) and the complementary structure (Figure 6C). The lenses produced show both good topography and coaxial alignment. The latter is apparent from the uniform retardance colour when viewed at 45° to crossed polarisers (Figure 6A,C) and the excellent dark state when parallel to the crossed polarisers (Figure 6B, D), confirming that the embossing process produces structures with very small or zero offset. The dark state in (Figure 6D) reveals a few imperfections that are most likely caused by the rubbing process for one of the lenses.

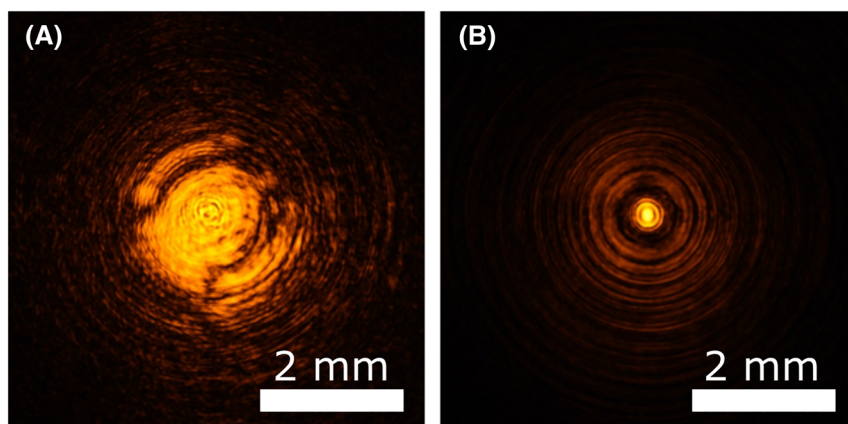


FIGURE 7 Transmission of laser beam (594 nm) through Fresnel zone cell on a charge-coupled device (CCD) camera at a distance of 20 cm from the lens: A, OFF-state and B, ON-state (10 V)

The empty, assembled cell (Figure 6E), where both substrates are rotated by 90° with respect to each other, shows a uniform bright state between crossed polarisers and independent of the orientation to the polarisers. This indicates that the good alignment of the RM was transferred to the index-matched liquid crystal in the TN configuration.

Figure 7 shows a collimated Gaussian 594-nm laser beam with circular polarisation transmitted through the Fresnel cell. In the OFF-state, the beam remains largely collimated but with some distortion due to reverse tilt and twist alignment errors in the filled lens after repeated switching (these defects are readily avoided using a long pitch chiral nematic with a handedness matched to the

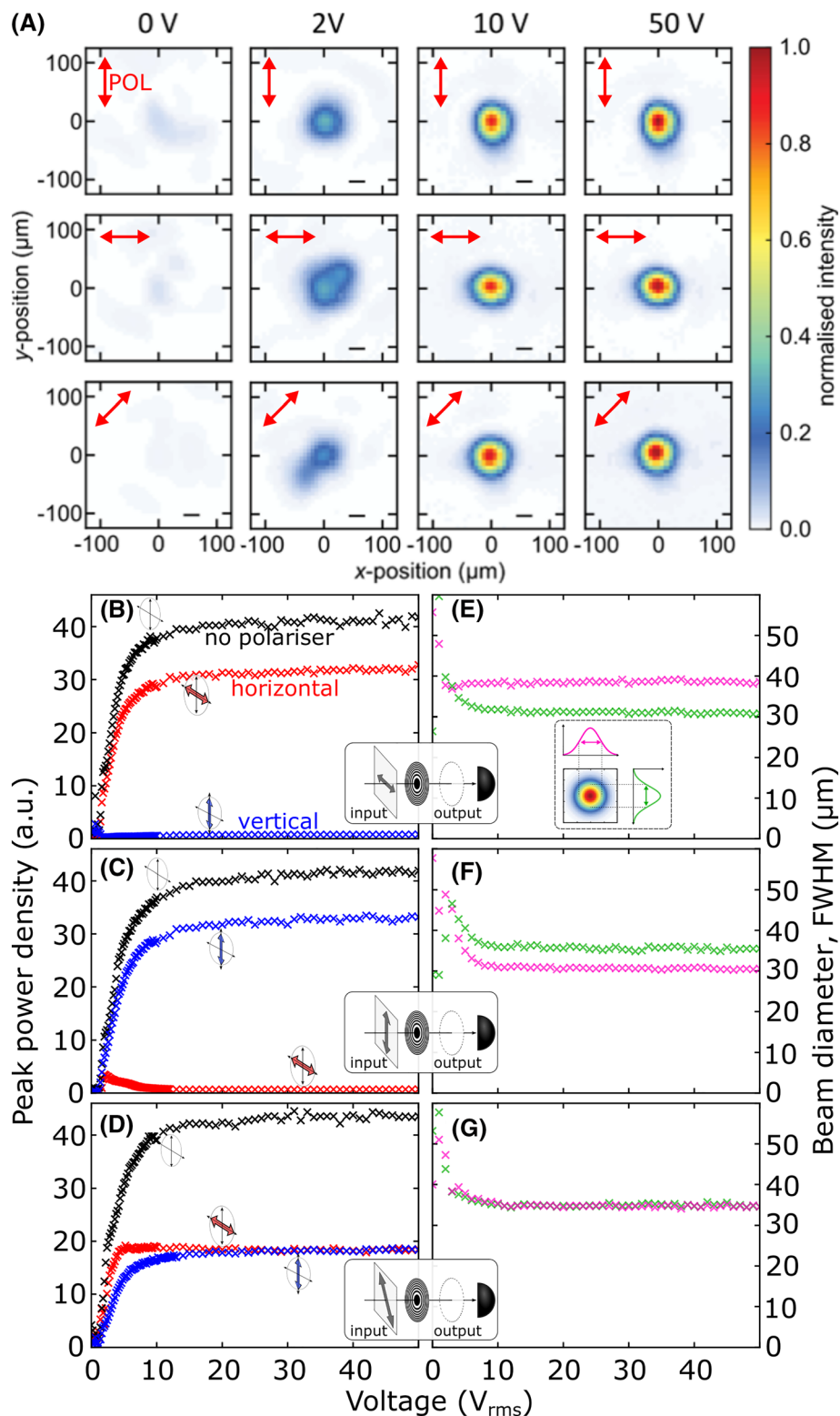


FIGURE 8 A, Beam profiles measured for different input polarisations (red arrow): vertical, horizontal, diagonal at different voltages. B-D, Peak intensity of central peak for different input and output polarisations as a function of voltage. E-G, Voltage-dependent spot diameter (full width at half maximum, FWHM) for different input polarisations (no output polariser)

pre-tilt on the lens surfaces in the method of Raynes²⁰). In the ON-state, light is focused in a central spot. Some of the power is distributed into concentric rings due to the Fresnel design, but the power focussed into the central spot was found to be over 33% of the input power at 10 V, which compares favourably with the 40% predicted theoretically. A more detailed investigation of the experimentally determined beam profile is shown in Figure 8A for different applied voltages. The input polarisation was controlled and adjusted to be horizontal, vertical, or diagonal to the principle optical axis of the lens cell (defined with respect to the first lens surface). At zero volts, there is no visible focussing, as explained in connection with A. A focal spot emerges as the voltages exceed the Fréedericksz transition and reaches over 33% efficiency

at 10 V. The focussing efficiency measured using an output polariser is summarised in Figure 8B-D, and the evaluation of the spot diameter is shown in Figures 8E-G. The focal spots of the field on state are slightly elongated along the axis of incident polarisation, which is caused by small imperfections of the liquid crystal alignment along the interstices of each Fresnel Zone in the embossed structure. This misalignment also leads to a loss of efficiency from the maximum possible theoretically from a 2-level diffractive lens (41%). The full-width-half-maximum of the focussed spot was 44 μm and 46 μm , for the horizontal and vertical polarisations, respectively, and this degree of ellipticity is considered small.

Cuts from the z-scans along the transverse (x or y direction) are given in Figure 9. The theoretical values

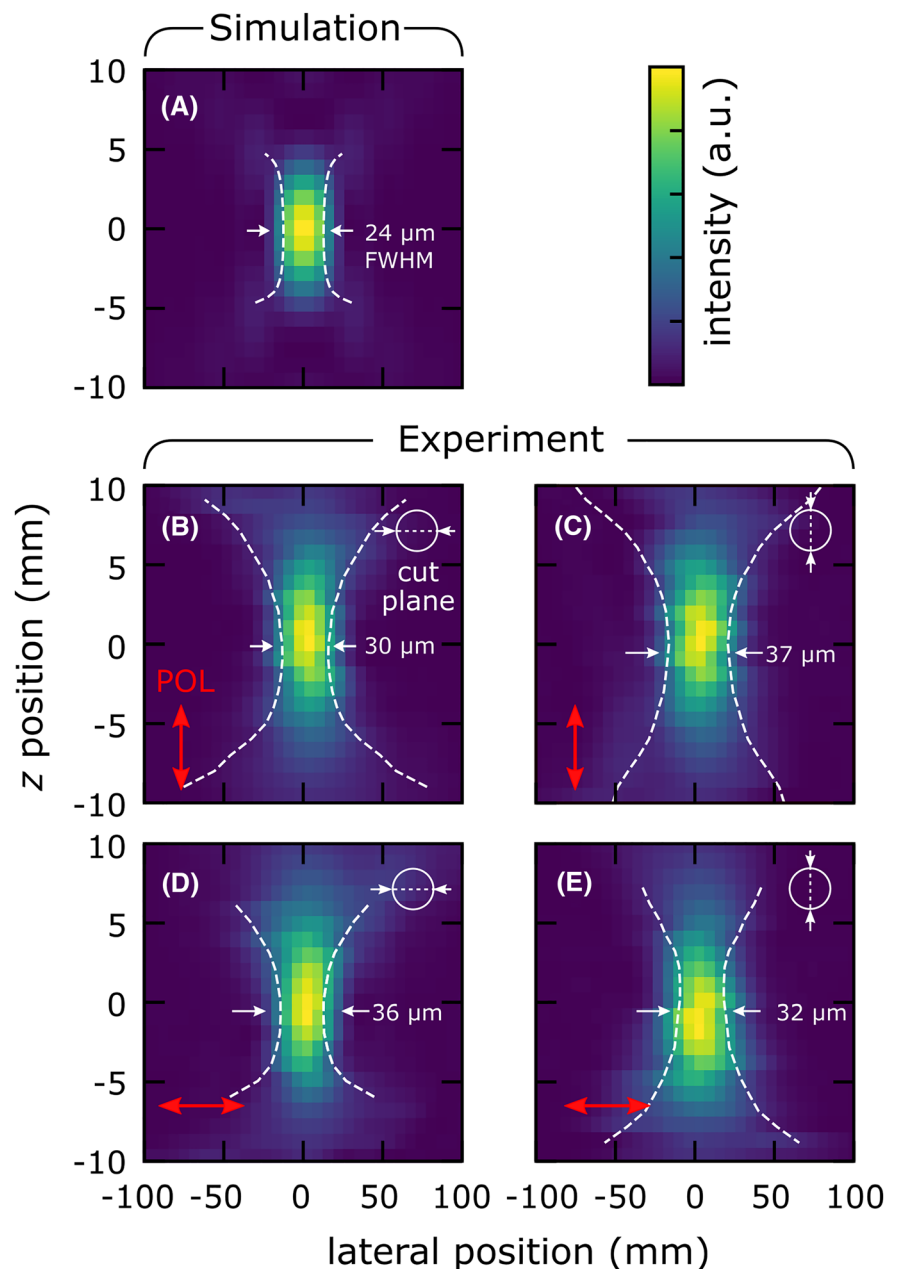


FIGURE 9 z-scans along the optical axis centred around the focal point. A, Theoretical simulation, B-E, experimental results for different input polarisations (red arrow) and cut along different directions (green)

were obtained by solving the Sommerfeld diffraction integral for a perfect 2-level phase plate and show a good match to those found experimentally. As discussed above, if the polarisation direction and the cut axis match, the spot size is slightly larger than for the orthogonal orientation.

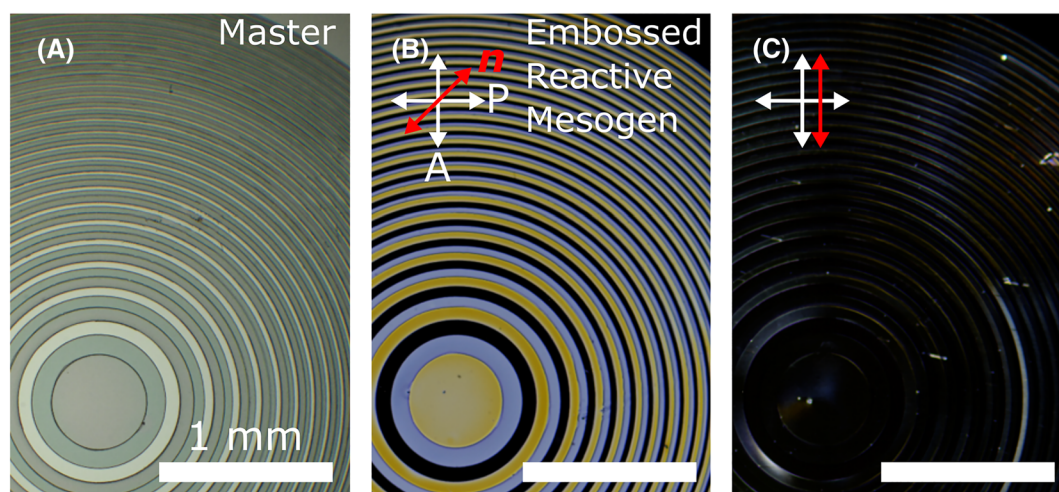
The 2-level lens design is inherently limited to about 41% efficiency. To overcome this, in the first step, we implemented a 3-level Fresnel lens as shown in Figure 10. The different birefringence colours in Figure 10B stem from the different thicknesses of the different Fresnel Zone rings. A device based on these substrates reaches in theory 68%. In the experiments, we found 55%, which we attribute to nonideal thickness of the RM and some inaccuracies in alignment between the substrates and again at the Fresnel zone boundaries. The errors for both 2-level and 3-level lenses leads to a consistent 20% loss. Hence, we predict that lenses with efficiencies in excess of 70% shall be possible using 5-level lenses.

A step further, which is currently under development, is the use of analogue Fresnel lenses. This gives a potential efficiency of 100% if shadow effects are ignored. Refractive Fresnel lenses are expected to change focal length with varying voltage, which contrasts the diffractive lenses, for which the efficiency is modulated. To this end, Figure 10D,E shows a 5-mm-diameter embossed refractive Fresnel lens between crossed polarisers, which successfully gave polarisation independent switching in both the quiescent and fully switched states.²¹

5 | IMPACT FOR USE IN SWITCHABLE CONTACT LENSES

For the design to be suitable for use in contact lenses, the lens structure must be of a refractive type, to avoid chromaticity. Use of refractive lenses also minimises any

Diffractive 3-Level Fresnel Lens



Refractive Fresnel Lens

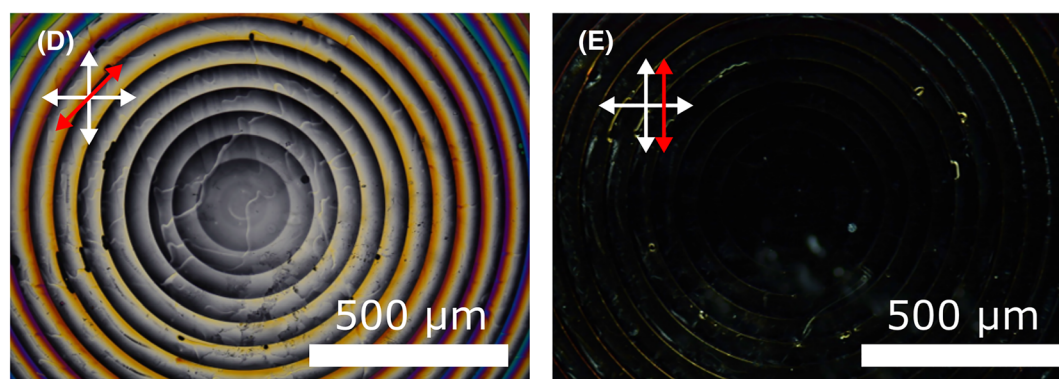


FIGURE 10 A, Micrograph of isotropic master of 3-level diffractive Fresnel lens with 5-mm diameter. B, C, Polarising optical micrograph of anisotropic embossed copy of the lens between crossed polarisers in, B, 45° and, C, parallel to one of the polarisers. D, E, Embossed refractive Fresnel lens between crossed polarisers. To aid visibility, the camera exposure time for E) is 10x that of D)

differences in upper and lower lens efficiencies for off axis light. For a meniscus contact lens of the design shown in Figure 1, the birefringent refractive lens will typically have maximum thicknesses of 25 μm to achieve the required +2.5D correction.⁶ Of course, this leads to a significant voltage drop across the polymer in the centre of the lens for a positive meniscus lens and at the outer edge of a negative meniscus lens. In this geometry, it is also important to set the cell gap high, towards the Mauguin limit, so that the TN guiding effect is independent of the varying gap of the meniscus lens. This means that any increase in operating voltage can be kept small, albeit with a slower response. Alternatively, the conductive layer must be deposited onto the RM layer, in which case extra alignment layers are also required. This is the arrangement suggested in Figure 3C,D.

6 | CONCLUSIONS

A simple geometry and fabrication method are proposed that provide superior operation of polarisation independent lenses. This design is applicable to a multitude of optical structures, from switchable gratings and prisms, to high efficiency lenses. In addition to its use in contact lenses, other early adopters or this technology are likely to be adaptive lenses for digital camera eyepieces and cell-phones. Of course, for an application such as contact lenses, there remain a series of technical challenges. Not least amongst these is the miniaturisation of the switching electronics to ensure that the lens retains its cosmetic appeal. Also, the market for hard-contact lenses made from plastics such as PMMA is diminishing, as users prefer semi-permeable, soft of hybrid lens materials. However, progress in transparent and flexible electronics²² is progressing at great speed, driven by the internet-of-things, smart textiles, and medical technologies.

ACKNOWLEDGMENTS

JCJ acknowledges the financial support from the UK's Engineering and Physical Sciences Research Council for an Advanced Fellowship in Manufacturing EP/L015288/2. MW wishes to thank Merck for funding under the *Leeds and Merck Project (LAMP)*. The authors wish to thank Merck KAaG in Darmstadt Germany, for the provision of the liquid crystal and RM materials. The authors also would like to thank Professors Phil Morgan (Manchester) and Helen Gleeson (Leeds), Tim Haynes (DVS) and Dr Owain Parry (Merck) for useful discussions.

ORCID

J. Cliff Jones  <https://orcid.org/0000-0002-2310-0800>

Markus Wahle  <https://orcid.org/0000-0002-2241-9975>

REFERENCES

- Sato S. Liquid-crystal lens-cells with variable focal length. *Jap J Appl Phys.* 1979;18:1679.
- Lin YH, Wang YJ, Reshetnyak V. Liquid crystal lenses with tunable focal length. *Liq Cryst Rev.* 2017;5(2):111–143.
- Ishihara S, Kobayashi S, Ukai Y. High Quality Liquid Crystal Displays and Smart Devices; Volume 2: Surface Alignment, New Technologies and Smart Device Applications”, Stevenage, United Kingdom: Chapter 13. In: IET Books; 2019.
- Milton HE, Kaur S, Jones JC, Gleeson HF, Morgan PB, Clamp J. Liquid crystal device and method of manufacture, Priority date Aug 1, 2013. *Patent. US 10,459,128, B2*; 2019.
- Syed IM, Kaur S, Milton HE, et al. Novel switching mode in a vertically aligned liquid crystal contact lens. *Opt Express.* 2015; 23:9911–9916.
- Bailey J, Kaur S, Morgan PB, Gleeson HF, Clamp J, Jones JC. Design considerations for liquid crystal contact lenses. *J Phys D Appl Phys.* 2017;50(48):485401.
- Bailey J, Morgan PB, Gleeson HF, Jones JC. Switchable liquid crystal contact lenses for the correction of presbyopia. *Crystals.* 2018;8(1): 29.
- Galstian T, Sova O, Asatryan K, Presniakov V, Zhhrabyan A, Evensen M. Optical camera with liquid crystal autofocus lens. *Opt Express.* 2017;25(24):29945.
- Strassburger H, Rentschler I, Jüttner M. Peripheral vision and pattern recognition: A review. *J Vis.* 2011;11(5):13. 1-82
- Ye M, Sato S. Liquid crystal lens of two liquid crystal layers. *Mol Cryst Liq Cryst.* 2004;422(1):197–207.
- Ye M, Wang B, Sato S. Double-layer liquid crystal lens. *Jpn J Appl Phys.* 2004;43(3A):L352–L354.
- Saito M, Maruyama A, Fujiwara J. Polarization-independent refractive-index change of a cholesteric liquid crystal. *Optical Mater Express.* 2015;5(7):1588–1597.
- Lin YH, Chen HS, Lin HC, Tsou YS, Hsu HK, Li WY. Polarizer-free and fast response microlens arrays using polymer-stabilized blue phase liquid crystals. *Appl Phys Lett.* 2010;96 (11):113505.
- Li Y, Wu ST. Polarization independent adaptive microlens with a blue-phase liquid crystal. *Opt Express.* 2011;19(9):8045–8050.
- Wang X-Q, Srivastava AK, Chigrinov VG, Kwok, H- S. Switchable Fresnel lens based on micropatterned alignment. *Opt Lett.* 2015;38(11):1775–1777.
- Wahle M, Snow B, Sargent J, Jones JC. Embossing reactive mesogens: a facile approach to polarisation-independent liquid crystal devices. *Adv Opt Mat.* 2019;7(2):1801261.
- Amos RM, Bryan-Brown GP, Wood EL, Jones JC, Worthing PT. Embossing method and apparatus, May 13, 2002. *Patent US 7,824,516, B2*; 2010.
- Jones JC. Zenithal bistable displays: from concept to consumer. *J SID.* 2008;16(1):143–154.
- Jones JC. Defects, flexoelectricity and RF communications: the ZBD story. *Liq Cryst.* 2017;44(12):2133–2160.
- Raynes EP. Improved contrast uniformity in twisted nematic liquid-crystal electro-optic display devices. *Electron Lett.* 1974; 10(9):141–142.
- Wahle M, Wyatt P, Snow B, Sargent J, Parry O, Jones JC. to be published.
- Trung TQ, Lee N-Q. Materials and devices for transparent stretchable electronics. *J Mat Chem C.* 2017;5:2202–2222.

AUTHOR BIOGRAPHIES



Prof Cliff Jones, FEng, FInstP, FRSC, FRSA is an Engineering and Physical Sciences Research Council (EPSRC) Fellow for Advanced Manufacturing in the Soft Matter Physics Group at Leeds University working mainly on liquid crystal device physics. This follows a 30-year career in industrial research, firstly as Technical

Leader of the Displays Group at *DERA Malvern*, and then as founder and chief technology officer (CTO) of the spin-out company *ZBD Displays Ltd* (now *Displaydata*). He has won numerous awards, including the *Katherine Burr Blodgett* and *Charles Vernon Boys* Medals from the Institute of Physics, the *Gray Medal* and *Hilsum Medal* from the *British Liquid Crystal Society*, the *Sturgeon Medal* from the *Society for Information Display*, and the *Ernst and Young Science and Technology Entrepreneur of the Year*. As well as publishing over 120 papers in the field of liquid crystals, he is a prolific inventor with over 60 granted patent families. Since joining Leeds in 2015, he has co-founded *Dynamic Vision Systems Ltd* to commercialise switchable contact lenses. Prof Jones has been a Senior Member of the *Society for Information Display* since May 2010.



Dr Markus Wahle studied chemistry at the University of Paderborn, Germany, where he received his PhD working on micro-structured optical fibres and liquid crystals in early 2017. From July 2017 to July 2019, he was working at the University of Leeds as postdoctoral researcher for the Leeds and Merck Project (LAMP)

funded by Merck KGaA. Dr Wahle received the Young Researcher Award from the German Liquid Crystal Society in 2017 and the Young Scientist Award from the British Liquid Crystal Society in 2019. He has published more than 10 papers related to optics and liquid crystals in journals such as *Optics Letters* and *Advanced Optical Materials*. Since July 2019, Dr Wahle is working as a development engineer for optics in satellites and space-related devices at OHB System AG in Munich, Germany.



Dr James Bailey is a Senior Scientist at Dynamic Vision Systems which he joined in 2018, where he is responsible for optical design and fabrication. He earned his PhD from the University of Nottingham in 2014 in Polymer Photonics. He joined the University of Manchester's liquid crystal group later in 2014, as a postdoctoral

research fellow, and followed the group to the University of Leeds in 2015. During that time, he had worked on nondisplay liquid crystal devices with Prof Cliff Jones. These devices included liquid crystal contact lenses that can electronically switch their focal power. James is a specialist in designing and building challenging optical devices. This includes building equipment to assist with manufacturing and characterisation of liquid crystal contact lens prototypes.



Tom Moorhouse is a Scientist at Dynamic Vision Systems which he joined in 2018. Previously, Tom completed his MPhys at Leeds University, with his final year Masters working on the alignment of liquid crystal displays. His responsibilities now include developing bespoke equipment for lens preparation and device assembly and the

manufacturing of contact lens substrates using conventional commercial methods.



Dr Benjamin Snow is a Doctor of Optical Engineering and a senior research scientist working at Merck Chemicals Ltd, a subsidiary of Merck KGaA. Ben completed both his PhD in Optoelectronics (2011) and undergraduate studies (2006) at the University of Southampton. His university research included adaptive waveguide

architectures, liquid crystal defect dynamics, and reconfigurable telecommunications systems. His current research ranges from novel liquid crystal display modes to waveguide optics, optical gratings and holography.



Joe Sargent worked as R&D Manager at Merck Chemicals Ltd, a subsidiary of Merck KGaA from 2007. He graduated with a Master's Degree in Physics from the University of Southampton in 2006. Managing an international team of researchers supporting multiple customer projects on liquid crystal and reactive mesogen materials for digital optics applications. Joe is the inventor of six granted US patents.

How to cite this article: Jones JC, Wahle M, Bailey J, Moorhouse T, Snow B, Sargent J. Polarisation independent liquid crystal lenses and contact lenses using embossed reactive mesogens. *J Soc Inf Display*. 2020;1–13. <https://doi.org/10.1002/jsid.874>